CLM - P 423

This document is intended for publication in a journal, and is made available on the understanding that extracts or references will not be published prior to publication of the original, without the consent of the authors.

CLM - P 423

UKAEA RESEARCH GROUP

Preprint

PULSE PROPAGATION IN CO_2 LASER AMPLIFIERS

E ARMANDILLO
I J SPALDING

CULHAM LABORATORY
Abingdon Oxfordshire

1975

CLM-P 423

PULSE PROPAGATION IN CO_2 LASER AMPLIFIERS

E. Armandillo and I.J. Spalding

Culham Laboratory, Abingdon, Oxon, OX14 3DB, UK
(Euratom/UKAEA Fusion Association)

ABSTRACT

Numerical predictions of pulse amplification in atmospheric CO_2 laser amplifiers are discussed. A conventional 4-temperature kinetic model is first used (with a self-consistent electron-beam source term) to establish the kinetic temperatures of relevant CO_2 vibrational levels in a pumped amplifier of arbitrary gas composition and pressure. The power amplification of a (single-line) pulse of arbitrary duration propagating through this amplifier is then examined in the simplifying approximation that N_2-CO_2 relaxation can be neglected. The treatment includes multi-level (rotational and vibrational) energy exchange, and Fermi coupling between the 100 and 02^00 levels. Coherent effects, of importance for sub-nanosecond propagation, are handled with terms including the dipole-dephasing time τ_2. Asymptotic pulse shapes are observed.

....

(Submitted for publication in J.Phys.D, Appl.Phys.)

July, 1975.

1. INTRODUCTION

Theoretical studies of pulse amplification in electron-beam (eb) pre-ionised CO_2 laser systems have been previously published by several authors. The problem was first treated in a multi-temperature kinetic (Boltzmann) approximation, in which characteristic temperatures are assigned to -

(a) (He-N_2-CO_2) gas translation, (T_g)

(b) the nitrogen vibrational mode, (T_{N_2})

(c) the anti-symmetric (ν_3) CO_2 stretch mode, (T_{ν_3}), and

(d) a lower CO_2 lasing level, in which the bending (ν_2) and symmetric stretch (ν_1) modes are assumed to be in equilibrium ($T_{\nu_2} = T_{\nu_1}$).

Temperature-dependent electronic excitation-rate coefficients are required as input parameters for this four-temperature kinetic (4TK) model, which has been reviewed by Harrach and Einwohner (1973), among others.

For high peak-power applications, amplifiers operating at pressures of one atmosphere or greater are required (Beaulieu 1970); electrical excitation is then normally accomplished in pumping times of less than 10 μs, so that excitation energy is not unduly wasted by collisional de-excitation of the upper lasing level, ν_3. For laser pulse durations (τ_p) considerably exceeding the CO_2 dipole-dephasing time (τ_2) pulse propagation through the laser medium can be adequately described in the rate equation approximation, provided the following effects are correctly handled as the duration is successively shortened:*

(a) $\tau_p \lesssim 1$ μsec decoupling of $CO_2(\nu_3)$ from N_2 vibrational levels.

(b) $\tau_p \lesssim 10$ nsec, decoupling of the Fermi-resonant CO_2 ν_2 and ν_1 lower levels (on a time-scale τ_F), and higher levels of the ν_3 mode (on a time-scale τ^3_{vv})

(c) $\tau_p \lesssim 0.2$ nsec decoupling of the rotational j levels (with a characteristic time $\tau_R{}^j, \tau_R{}^{j-1}$, respectively, for the upper and lower lasing level).

The amplification of nanosecond pulses has been discussed by Stark et al (1973), Figuera et al (1973), Feldman (1973) and Ballick et al (1975). The purpose of the present paper is to describe a computer model which has been used to handle pulses of arbitrary duration in eb CO_2 amplifiers of specified but variable gas composition and pressure, in the limit that dispersion effects can be neglected. In particular Fermi-resonance between the ν_2 and ν_1 modes, intramode energy exchange processes and, for shorter (sub-nanosecond) pulses, coherent effects which occur when $\tau_p \lesssim \tau_R{}^j, \tau_R{}^{j-1}$ are treated explicitly for the CO_2 system. (Some of these effects have been treated implicitly for generalised, high gain, molecular amplifiers by Hopf and Rhodes (1973) and Hopf (1974)).

2. PULSE PROPAGATION MODEL

2.1 Collisional Model

In atmospheric CO_2 laser amplifiers the spectral lines are homogeneously broadened, with a dipole-dephasing time (τ_2) related to the (Lorentzian)

---

* The time scales indicated are appropriate to typical CO_2 laser gas mixtures, at atmospheric pressure.

bandwidth B_f by the expression

$$\tau_2 = \frac{1}{\pi B_f} . \qquad \ldots (1)$$

The value of τ_2, which is an averaged collision time, is dependent on the gas composition and total pressure; it will therefore be convenient to illustrate quantitative results for a typical medium having a $He:N_2:CO_2$ composition of 3:1:2 at 1 standard atmosphere. The lasing levels, involving for example the P (20) transition, are immersed in a rotational reservoir whose population is Boltzmann distributed at the gas temperature T_g, in the absence of any perturbing field. The vibrational levels, say (0,0,1), are in turn immersed in a vibrational reservoir, say (0,0,k) having a Boltzmann distribution appropriate to the (pumped) temperature - in this case T_{ν_3}: this assumption has been the essence of the 4TK model. The influence of the rotational reservoir is now introduced into the dynamics of the jth rotational level by terms of the form

$$\left.\frac{\delta N_j}{\delta t}\right|_{\text{collisions}} = -\sum_k W_{jk} N_j + \sum_k W_{kj} N_k \quad \text{for all } k \neq j \qquad \ldots (2)$$

where '$W_{m,n}$' is the rate constant for the transition "$m \rightarrow n$". It follows from the principle of detailed balance that

$$\left.\frac{\delta N_j}{\delta t}\right|_{\text{collisions}} = -\sum_k \frac{N_k^e N_j}{\tau'_{jk}} + \sum_k \frac{N_j^e N_k}{\tau'_{jk}} \qquad \ldots (3)$$

where $\tau'_{jk} = \tau'_{jk} = \frac{N_j^e}{W_{kj}} = \frac{N_k^e}{W_{jk}}$ and N_i^e is the equilibrium population density of the ith level. Assuming the following relation to hold

$$W_{jk} = W_{jk}^* \cdot \frac{N_k^e}{N_{k*}^e} \qquad \ldots (4)\dagger$$

† From (4) onwards, j will be reserved to represent the level of highest gain; then the approximation (4) implies that rotational relaxation is slower for collisions in which $\Delta j > \pm 2$ (see Jacobs et al 1974)

where k^* is the level closest to j (i.e. $k^* = j \pm 2$), equation (3) becomes

$$\left.\frac{\delta N_j}{\delta t}\right|_{collision} = -(N_j - z_j N_v)/\tau_k^j \qquad \text{...(5)}$$

where z_j, the rotational Boltzmann partition function,

$$\frac{N_j^e}{N_v^e} = \frac{hcB(2j+1)}{kTg} \cdot \exp-[hcBj(j+1)/kTg] \; .$$

N_v^e is the total vibrational population and τ_R^j is the time constant for relaxation of the jth lasing level to all other rotational levels i.e. $\tau_R^j = (\sum_k W_{jk})^{-1}$ for all $k \neq j$. Note that the time constant for the inverse transition $k \rightarrow j$ in this model is given by

$$\tau' \equiv (W_{kj})^{-1} = (W_{ij})^{-1} \; \forall i,k \neq j \; .$$

Whence it is easily seen that

$$\frac{\tau_R^j}{\tau'} = \frac{W_{kj}}{\sum_k W_{jk}} = z_j \; . \qquad \text{...(6)}$$

Thus the rate of rotational supply to the jth (perturbed) level proceeds more slowly than the inverse process, taking a characteristic time of $(\tau_R^j/z_j) \sim 2.5$ nsec at 1 atmosphere.

The intramode vibrational reservoir can be treated in a similar manner, leading to a rate equation of the form

$$\left.\frac{\delta N_v}{\delta t}\right|_{collisions} = -(N_v - z_\nu N_\nu)/\tau_{vv} \qquad \text{...(7)}$$

where N_v refers to the vibrational level in question, say (0,0,1), N_ν refers to the modal population, say $\sum_k N(0,0,k)^*$, and τ_{vv} is the time constant for the exchange of a vibrational quantum in that mode. The vibrational

---

* Here, and in what follows, mixed states of the type $(i,j+j',k)$ have not been considered since the occupation probability is generally lower than for the pure states.

functions ($Z_\nu \equiv N_v{}^e/N_\nu{}^e$) assume the following values for the ν_1, ν_2, ν_3 modes respectively -

$$Z_{\nu_3} = r(1-r) \qquad \ldots(8)$$

$$Z_{\nu_2} = s^2(1-s)^2 \qquad \ldots(9)$$

$$Z_{\nu_1} = s^2(1-s^2) \qquad \ldots(10)$$

where r and s are appropriate Boltzman factors -

$$r = \exp(-\hbar\omega_{\nu 3}/kT_{\nu 3}) \qquad \ldots(11)$$

$$s = \exp(-\hbar\omega_{\nu 2}/kT_{\nu 2}) \,. \qquad \ldots(12)$$

Thus,

$$\left.\frac{\delta N_{001}}{\delta t}\right|_{coll} = -\,(N_{001} - z_{\nu_3} N_{\nu_3})/\tau_{vv}^{3} \qquad \ldots(13)$$

$$\left.\frac{\delta N_{100}}{\delta t}\right|_{coll} = -\,(N_{100} - z_{\nu_1} N_{\nu_1})/\tau_{vv}^{1} \,. \qquad \ldots(14)$$

It follows from (13) that the time required to supply vibrational energy to the perturbed (0,0,1) level is of order ($\tau_{vv}{}^3/z_{\nu_3}$) $\gtrsim$ 10 nsec at 1 atmosphere, and therefore the inclusion of the intramode reservoir, even in the present approximate treatment, should be important for pulse durations of this order.

Fermi coupling between the (1,0,0) and ($0,2^0,0$) levels may be

---

* The Boltzman factor for the mode ν_1 is $e^{-\hbar\omega_{\nu 1}/kT_{\nu_1}} \simeq e^{-2\hbar\omega_{\nu_2}/kT_{\nu_2}} = s^2$ since $\nu_1 \simeq 2\nu_2$ and $T_{\nu_1} \equiv T_{\nu_2}$, before propagation of the pulse.

introduced in a similar manner: it is postulated that the vibrational temperatures and populations of these two levels are nearly equal, since the pumping is relatively slow. If any perturbation should upset this equilibrium, collisions will tend to restore the initial conditions on the time scale τ_F. Hence, for the lower vibrational levels:

$$\left.\frac{\delta N_{100}}{\delta t}\right|_{coll} = - \frac{N_{100} - z_{\nu_1} N_{\nu_1}}{\tau_{vv}^1} - \frac{N_{100} - N_{020}}{\tau_F} \qquad \ldots(15)$$

$$\left.\frac{\delta N_{020}}{\delta t}\right|_{coll} = - \frac{N_{020} - N_{100}}{\tau_F} - \frac{N_{020} - z_{\nu_2} N_{\nu_2}}{\tau_{vv}^2} . \qquad \ldots(16)$$

2.2 Effect of Perturbing Fields

For an EM wave travelling along the 'z' axis the electric field component is given by

$$E(x,j,Z,t) = \mathcal{E}(x,j,Z,t)\exp[\ (wt-\beta Z)] \qquad \ldots(17)$$

where $\mathcal{E}$ is a complex number with a polarization vector directed along x, say, in the normal 'Z' plane. The field-driven polarization is expressed by the analogous relation

$$P(x,y,z,t) = \mathcal{P}(x,y,z,t)\exp[j(\omega t-\beta z)] \qquad \ldots(18)$$

where β $(= \omega n/c)$ is the real part of the wave number, and n is the refractive index of the medium, which is initially isotropic.

To simplify the present discussion transverse variations of the electric field, as well as processes like self-focusing and defocusing that can be handled through the inclusion of the non-linear dependence of n on E, have not been included: these effects will be discussed elsewhere. Working in the usual frame of the slowly varying envelope approximation (S.V.E.A), after the following change of coordinates

$$\begin{cases} z^i = z \\ \tau = t - zn/c \end{cases}$$

the Maxwell field equation reduces* to

$$\frac{\delta \mathcal{E}}{\delta Z} = -i \frac{\omega \mathcal{P}}{2\epsilon_0 cn} - k\mathcal{E} \qquad \ldots (19)$$

where the term '$k\mathcal{E}$' has been introduced phenomenologically to account for the field losses. Similarly, the dipolar equation becomes

$$\frac{\delta \mathcal{P}}{\delta \tau} = -\frac{\mathcal{P}}{\tau_2} + i \frac{p^2}{\hbar} \mathcal{E}(N_{001}^{J} - N_{100}^{J+1}) \qquad \ldots (20)$$

where p is the dipole matrix element, the value of which is tabulated with other relevant parameters in Appendix 1. The complete set of coupled-amplitude complex equations is summarized, for ease of reference, in Appendix 2. These equations, together with the time variation of the Boltzmann factors on the tens of nanosecond time scale, provide a self-consistent model of pulse propagation for pulse lengths ranging between several hundred nanoseconds to fractions of a nanosecond at intensities which can vary from very low levels to well above saturation, but not non-linear, levels. (For extremely short pulses, the question of orientational degeneracy arises. Hopf and Rhodes, 1973, conclude that it is not of practical importance.)

2.3 Numerical Technique

A Fortran 4 program was used for the numerical integration of the coupled equations in Appendix 2 and some typical results are discussed below. The program uses a conventional Simpson integration formula, swept on a two-dimensional grid. A detailed description of the code will be given in a subsequent Culham report.

---

* For details of the field-dipole coupled equation see, for example, Pantell and Puthoff (1969).

3. NUMERICAL RESULTS

3.1. Initial Conditions

The four-temperature kinetic code is first used, with a self-consistent electron-beam source term, to establish the temperatures of relevant CO_2 vibrational levels (including higher anti-symmetric stretch modes) in the pumped amplifier. Spatial variations in laser gain parameters along and transverse to the electron beam direction, which may arise in real systems, can be handled but are neglected here for simplicity. It is assumed that the system is electrically pumped on a time-scale of a few microseconds. The 4 TK code thus computes a set of initial conditions, in order that the power amplification of a (single-line) pulse propagating along the pumped amplifier can subsequently be examined. Table I illustrates a few calculations made with this code, and compares the predicted peak small-signal gain coefficient (α_o), current density (J) and time to peak gain (τ_α) with those measured experimentally in (1) a small glow-gun pre-ionized experiment at Culham and (2) in cold-cathode experiments at Lawrence Livermore Laboratory (UCRL Report 50021-73-2 pp 154).

TABLE I

Computer Input					Prediction			Experiment		
Gas Mix $He:N_2:CO_2$	Sustainer Field E/N ($kV\ cm^2\ 10^{-17}$)	Electron Beam Specification			J ($A\ cm^{-2}$)	τ_α (μs)	α_o (cm^{-1})	α_o (cm^{-1})	τ_α (μs)	J A(cm^{-2})
		Current (mA/cm^2)	Energy (keV)	Duration (μs)						
3:1:1	13-17	≥ 33	100	6	4-5	7	1.5%	1.6%$^{(i)}$	~ 4	5
3:1:2	15	680	190	2	27-32	2.8	4.1%	4.7%$^{(ii)}$	-	~32
3:1:2	18.5	200	150	5	19.23	4	5.0%	-$^{(iii)}$	-	-

Note: (i) Culham 1 m × 0.1 m glow-gun experiment. (Culham Progress Report CLM-PR16 and 17)

(ii) UCRL-50021-73-2 pp. 154.

(iii) Systems, Science and Software 2 m × 0.2 m cold cathode gun, being commissioned at Culham. $He:N_2:CO_2$ = 3:2:1 at 1 stand. atmos.

The most uncertain parameter in the input data is probably the recombination coefficient, which is taken to be a constant having a value of $\sim 1.10^{-7}$ $cm^3 sec^{-1}$ (Mills 1973), but which is expected to be temperature dependent (Bardsley and Biondi 1972). Line 3 describes computed parameters appropriate to a 200 cm x 20 cm x 20 cm amplifier now being commissioned at Culham, and Fig. 1 illustrates the computed time variation of (i) α_o (ii) electron density n_e (iii) stored optical energy and (iv) $T_{\nu 3}$ under the same assumed conditions. The pulse-propagation calculations discussed in § 3.2 will use this particular laser medium at its time of peak small-signal gain (α_o = 5% cm^{-1}) to define a set of initial conditions broadly representative of present state of the art high-power atmospheric CO_2 laser amplifiers. It should, perhaps, be stressed that these particular conditions have not been described in detail in any experimental publication, and that the present 4 TK prediction will be subject to normal experimental uncertainties in the rate coefficients and other input data tabulated in Appendix 1.

3.2. Pulse Propagation

As discussed in § 2.2, the computer code can handle a wide variety of input pulse shapes. Thus, for pulse rise times $\tau_o \leqslant 1$ ns (at 1 atmosphere) the energy extraction efficiency shows a very strong dependence on both the input pulse duration and energy, as might be expected for a two-level system. Due to field-driven inversions of the upper and lower lasing levels the pulse has a tendency to break-up, above a certain input pulse area $\theta_i = \frac{p}{\hbar} \int_{-\infty}^{\infty} E d\tau > \pi$ (see Hahn & McCall, 1969, for the language of self-induced transparency). The amplification of a truncated gaussian pulse having an input power $P_i = x\, e^{-x^2/2}$, where (retarded) time $\tau = x\, \tau_o$, is illustrated in Figure 2 for a pulse of rise time τ_o = 0.1 ns. The pulse shape after propagation through 1 m of the 3:1:2 ($He:N_2:CO_2$) α_o = 5% cm^{-1} gain medium is shown for input pulses of (a) 0.075, (b) 0.125 and (c) 0.25 J/cm^2. Also shown is the energy extraction efficiency (η), defined by the relation

$$\eta = \frac{W_o(\tau) - W_i(\tau)}{W_{Av}}$$

where $W_o(\tau)$ is the output energy after the time τ,

$W_i(\tau)$ is the input energy over the same time duration τ,

and W_{Av} is the available energy within the active gas volume V,

ie $$W_{Av} = \frac{\hbar\omega}{2} (N^{001} - N^{100}) V.$$

It will be seen that η decreases with increase of input energy, or decrease of τ_o.

Fig. 3 illustrates the amplification of a shorter pulse, for which $\tau_o = \tau_2 = 0.06$ ns, over the same range of energy densities. This pulse is more intense ($\theta_i > 3\pi$ at 0.25 J/cm^2), and suffers attenuation rather than amplification. After propagating several metres, ie a distance $>> 1/\alpha_o$, the pulse assumes a characteristic area of 3π, a result which appears to be independent of input energy or pulse duration and is related to theories of self-induced transparency. (Note that the area theorem is not normally applied to homogeneously broadened systems, cf Icsevgi and Lamb (1969)). The pulse splits into two components, an initial spike that tends to increase in intensity and decrease in total width (to a limiting value of $\sim \tau_2$), and a tail which decreases in intensity and increases in width as it propagates through the medium. Fig. 4 illustrates the propagation of a $\theta_i \sim 10\pi$ pulse over a distance of 5 metres, the area of the initial spike falls asymptotically to $\sim 3\pi$.

For pulses of somewhat longer duration, other levels within the molecular ensemble can smooth out population inversions driven by coherent EM propagation. In such situations the amplified pulse shows an initial spike, due to coherent two-level interactions, followed by a broad hump containing a major fraction of the energy. As the pulse propagates along the amplifier, the initial spike narrows to a width $\sim \tau_2$. The secondary hump develops a fine-structure having a frequency $\sim (1/\tau_2)$ and an asymptotic pulse shape, with a tail which is well approximated by the function $e^{-(Z_j \tau/\tau_R)}$ where z_j is defined in eqn (5). Figs 5 and 6 illustrate the pulse shape and energy extraction efficiency after propagation over 1 m for pulses having $\tau_o = 1$ and 2 ns respectively, at incident energy densities of (a) 0.075, (b) 0.125 and (c) 0.250 J/cm^2. Amplification of these longer pulses is, of course, quite different from the two-level situation, and the extraction efficiency increases with input energy and pulse duration. Indeed, when $\tau \gtrsim 10$ ns the energy extracted can exceed that stored in the (0, 0, 1) mode, due to replenishment from the higher asymmetric stretch levels discussed in § 2.1.

Finally, Fig. 7 shows the asymptotic pulse shape that develops along this high gain amplifier. The pulse assumes a characteristic shape which is in good qualitative agreement with the discussion by Hopf, 1974, of generalized molecular amplifiers.

ACKNOWLEDGEMENTS

The authors wish to thank Dr. S. Solimeno of the University of Naples for encouraging the present co-operation; E. Armandillo acknowledges receipt of a Euratom 'Borsa di perfezionamento scientifico' (Fellowship).

APPENDIX 1

VALUES OF SOME RELEVANT PARAMETERS ENTERING INTO THE MODEL

1.	Gas mixture	$He:N_2CO_2$	3:1:2
2.	Field to pressure ratio	E/P	5 kV/cm.atm.
3.	Pressure	P	1 atmosphere
4.	Exc. rate for the mode 'ν_1'	k_1	$1.1\times10^{-9} cm^3 sec^{-1}$
5.	Exc. rate for the mode 'ν_2'	k_2	$1.8\times10^{-9} cm^3 sec^{-1}$
6.	Exc. rate for the mode 'ν_3'	k_3	$1.6\times10^{-9} cm^3 sec^{-1}$
7.	Exc. rate for the N_2	K_N	$1.5\times10^{-9} cm^3 sec^{-1}$
8.	Transition	P(20)	10.5912 μm
9.	Matrix 'P' element	p	6.8×10^{-30} coul.cm
10.	Dipole dephasing time	τ_2	0.06×10^{-9} sec
11.	Rotat.time constant	$\tau_r^{\,j} = \tau_r^{\,j+1}$	0.15×10^{-9} sec
12.	Intramode time const.	$\tau^3_{vv} = \tau^2_{vv} = \tau^1_{vv}$	~~11.0×10^{-9} sec~~ 1×10^{-9} sec
13.	Fermi time const.	τ_F	10.0×10^{-9} sec
14.	Amplifier length		variable (cm)
15.	Amplifier cross section		20 cm x 20 cm

The following formulae have been used for the

a) FERMI RATE CONSTANT (Stark, 1973):

$$K_F=(1.42\pm0.5)10^5[P_{CO2}+0.46P_{N2}+0.054P_{HE}]\,sec^{-1}torr^{-1}$$

b) ROTATIONAL RATE CONSTANT (Jacobs et al, 1974)

$$K_R=1.10^7[(1.3\pm0.2)P_{CO2}+(0.6\pm0.1)P_{HE}+(1.2\pm0.2)P_{N2}]\,sec^{-1}torr^{-1}$$

c) P(20) LINE BROADENING COEFF (Abrams, 1974)

$$B_f=[(7.61\pm0.1)P_{CO2}+(5.58\pm0.2)P_{N2}+(4.88\pm0.18)P_{HE}]\,1.10^6\ Hz\ torr^{-1}$$

Corrigendum
to
CLM-P423
(issued September, 1975)

PULSE PROPAGATION IN CO_2 LASER AMPLIFIERS

by

E. Armandillo, I. J. Spalding

Will you please note the following correction:-
Appendix 1, item 12, page 12

delete: $\tau_{vv} = \tau^2_{vv} = \tau^1_{vv}$ 11.0x10^{-9} sec

insert: $\tau^3_{vv} = \tau^2_{vv} = \tau^1_{vv}$ 1 x 10^{-9} sec

U.K.A.E.A. Research Group,
Culham Laboratory,
Abingdon,
Oxon.

September, 1975

The rate of the intramode energy transfer, which is not exactly known(Burak and al., 1973), is of the order

$$K_{vv} \approx 1.10^{6} torr^{-1} sec^{-1}$$

(Since the present paper was written, Harrach (1975) has also discussed this intra-mode vv rate, with similar conclusions.)

The excitation rates, 4→7, have been obtained by numerically solving the Boltzmann equations for the cases of interest(Andrews, 1974, using Cross Sections discussed by Lowke et al, 1973).

APPENDIX 2

SUMMARY OF THE AMPLITUDE-COUPLED EQUATIONS

1. $$\frac{\delta N^{j}_{001}}{\delta\tau} = -\frac{N^{j}_{001} - z_j N_{001}}{\tau_R^{\,j}} - i[\tilde{\mathcal{E}}\tilde{\mathcal{P}}^* - \tilde{\mathcal{E}}^*\tilde{\mathcal{P}}]/4\hbar$$

2. $$\frac{\delta N^{j+1}_{100}}{\delta\tau} = -\frac{N^{j+1}_{100} - z_{j+1} N_{100}}{\tau_R^{\,j+1}} + i[\tilde{\mathcal{E}}\tilde{\mathcal{P}}^* - \tilde{\mathcal{E}}^*\tilde{\mathcal{P}}]/4\hbar$$

3. $$\frac{\delta N_{001}}{\delta\tau} = -\frac{N_{001} - z_{\nu 3} N_{\nu 3}}{\tau^{3}_{vv}} - i[\tilde{\mathcal{E}}\tilde{\mathcal{P}}^* - \tilde{\mathcal{E}}^*\tilde{\mathcal{P}}]/4\hbar$$

4. $$\frac{\delta N_{100}}{\delta\tau} = -\frac{N_{100} - z_{\nu 1} N_{\nu 1}}{\tau^{1}_{vv}} - \frac{N_{100} - N_{020}}{\tau_F} + i[\tilde{\mathcal{E}}\tilde{\mathcal{P}}^* - \tilde{\mathcal{E}}^*\tilde{\mathcal{P}}]/4\hbar$$

5. $$\frac{\delta N_{020}}{\delta\tau} = -\frac{N_{020} - N_{100}}{\tau_F} - \frac{N_{020} - z_{\nu 2} N_{\nu 2}}{\tau^{2}_{vv}}$$

6. $$\frac{\delta N_{\nu 3}}{\delta\tau} = - i[\tilde{\mathcal{E}}\tilde{\mathcal{P}}^* - \tilde{\mathcal{E}}^*\tilde{\mathcal{P}}]/4\hbar$$

7. $$\frac{\delta N_{\nu 2}}{\delta\tau} = -\frac{N_{020} - N_{100}}{\tau_F}$$

8. $$\frac{\delta N_{\nu 1}}{\delta\tau} = -\frac{N_{100} - N_{020}}{\tau_F} + i[\tilde{\mathcal{E}}\tilde{\mathcal{P}}^* - \tilde{\mathcal{E}}^*\tilde{\mathcal{P}}]/4\hbar$$

9. $$\frac{\delta\tilde{\mathcal{P}}}{\delta\tau} = -\frac{\tilde{\mathcal{P}}}{\tau_2} + i\,\frac{p^2}{\hbar}\tilde{\mathcal{E}}[N^{j}_{001} - N^{j+1}_{100}]$$

10. $$\frac{\delta\tilde{\mathcal{E}}}{\delta z} = -k\tilde{\mathcal{E}} - i\,\frac{\omega}{2\epsilon_o c n}\tilde{\mathcal{P}}$$

where 'i' is the imaginary unity.

These equations can be simplified when considering the following restricted regimes of pulse duration (τ_p):

(a) $10 \text{ nsec} < \tau_p \lesssim \text{hundreds of nsec.}$

then $\frac{\delta}{\delta\tau} < 1/\tau_2, 1/\tau_R, 1/\tau_{vv}, 1/\tau_F$ so the time derivatives of $\mathcal{G}$, N^j_{001}, N^{j+1}_{100} can be neglected-allowing the equations to be rewritten in a more compact form.

(b) $\tau_{vv} < \tau_p \lesssim 10 \text{ nsec}$

then $\frac{\delta}{\tau} < 1/\tau_2$, so the time derivatives of $\mathcal{G}$ can be neglected.

(c) $\tau_R \lesssim \tau_p \lesssim \tau_{vv}$

here only the rotational reservoir is significant, so that intra-mode processes can be neglected.

(d) $\tau_p < \tau_R$

then $\frac{\delta}{\delta\tau} > 1/\tau_{vv}, 1/\tau_F, 1/\tau_R$ and the equations reduce to the well-known two-level coupled amplitude complex equation.

It is important to point out that in the regimes (a) and (b) the time variation of the Boltzmann factors entering into the vibrational functions $z_{\nu_3}, z_{\nu_2}, z_{\nu_1}$ must be added, in order to close the system of equations; such further equations are not discussed here. (For details, see Harrach & Einwohner, 1973).

REFERENCES

ABRAMS R L 1974 Appl.Phys.Lett. 25 609-611

ANDREWS K J 1974, University of Hull (Private communication)

BALLIK E A, GARSIDE B K and REID J 1975 Appl.Phys.Lett. 26 380-82

BARDSLEY J N and BIONDI M A 1970 Adv.Atom.and Mol.Phys. VII 1-57 (Academic Press, New York - London)

BEAULIEU A J 1970 Appl.Phys.Lett. 16 504-5

BURAK I, NOTER Y and SZOKE A 1973 IEEE J.Quantum Electron. QE-9 541-44

FELDMAN B J 1973 IEEE J.Quantum Electron. QE-9 1070-78

FIGUERA J F, REICHELT W H, SCHAPPERT G T, STRATTON T F and FENSTERMACHER C A 1973 Appl.Phys.Lett. 22 216-18

HAHN E L and McCALL S L 1969 Phys.Rev. 183 457-85

HARRACH R J and EINWOHNER T H 1973 Lawrence Livermore Laboratory Report UCRL-51399

HARRACH R J 1975 Lawrence Livermore Laboratory Preprint UCRL-76224 Rev.I

HOPF F A 1974 'Physics of Quantum Electronics' Vol.I ed. S. Jacobs, M. Sargent and M.O. Scully, Addison-Wesley Pubs.Inc., Reading (Mass)

HOPF F A and RHODES C K 1973 Phys.Rev. A8 912-29

ICSEVGY A and LAMB W E jr 1969 Phys.Rev. 185 517-45

JACOBS R R, PETTIPIECE J K and THOMAS S J 1974(a) Appl.Phys.Lett. 24 375-77

JACOBS R R, THOMAS S J and PETTIPIECE K J 1974(b) IEEE J.Quantum Electron. QE-10 480-86

LOWKE J J, PHELPS A V and IRWIN B W 1973 J.Appl.Phys. 44 4664-71

MILLS C B 1973 Los Alamos Report LA-5151 MS

PANTELL R H and PUTHOFF H E 1969 'Fundamentals of Quantum Electronics' J. Wiley and Sons, New York

STARK E E jr 1973 Appl.Phys.Lett. 23 335-37

STARK E E jr, REICHELT W H, SCHAPPERT G T and STRATTON T F 1973 Appl.Phys. Lett. 23 322-24

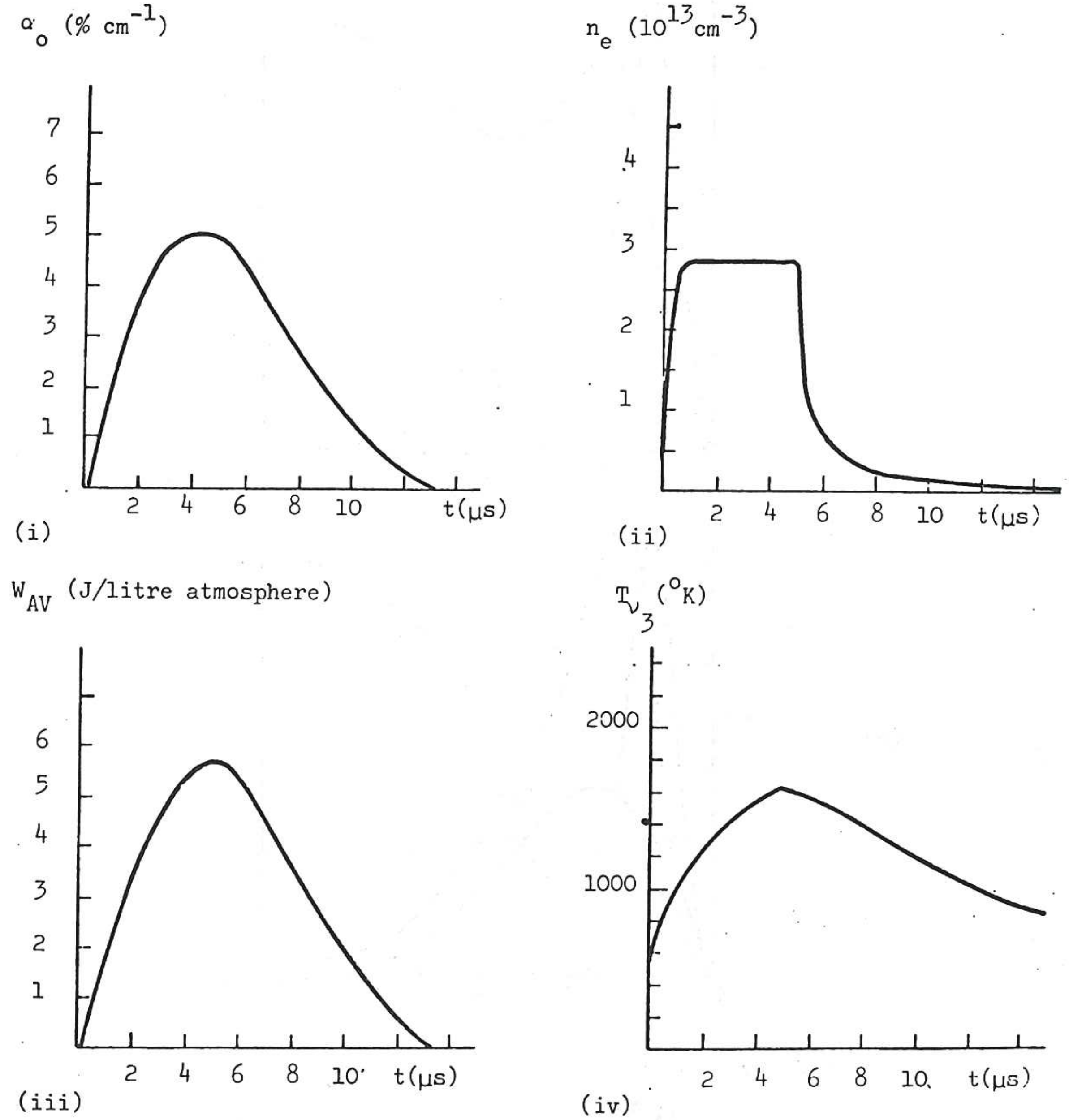

FIG.1 Predicted variation of (i) small signal gain (α_o), (ii) electron density (n_e), (iii) optical energy (W_{Av}) and (iv) T_{ν_3} at various times (t) after application of a 5 μs, 0.2 amp cm^{-2}, 150 kV eb pulse to the laser medium detailed in Appendix 1.

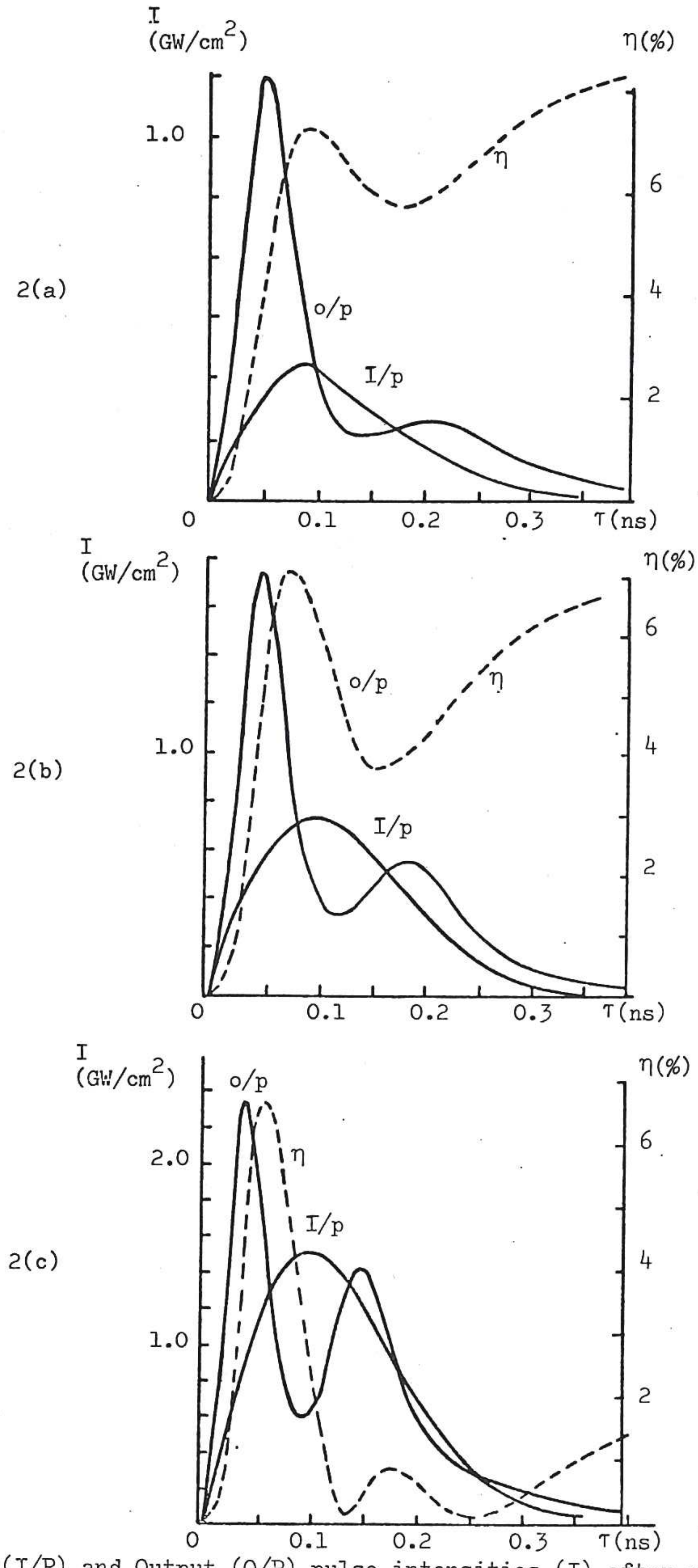

FIG.2 Input (I/P) and Output (O/P) pulse intensities (I) after propagation along a distance L = 1 metre of the $\alpha_o = 0.05\ m^{-1}$ medium detailed in Appendix 1 and Fig.1, for input energy densities of (a) 0.075, (b) 0.125, (c) 0.25 J/cm^2. Input pulse rise time $\tau_o = 0.1$ ns; extraction efficiency η shown as dashed line.

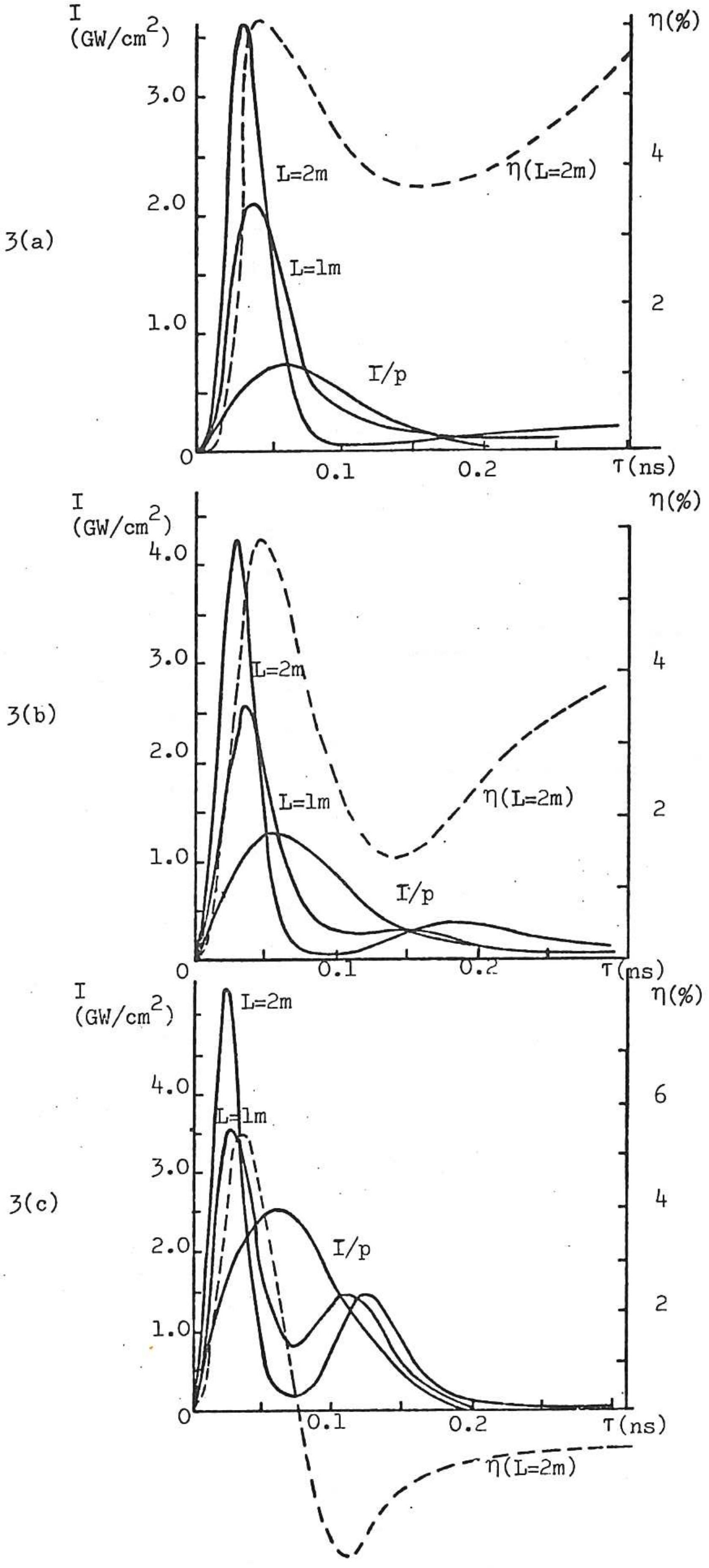

FIG.3 Output at L = 1m and L = 2m for τ_o = 0.06 ns; other conditions as Fig.2, viz I/P energy densities (a) 0.075, (b) 0.125, (c) 0.25 J/cm^2, etc.

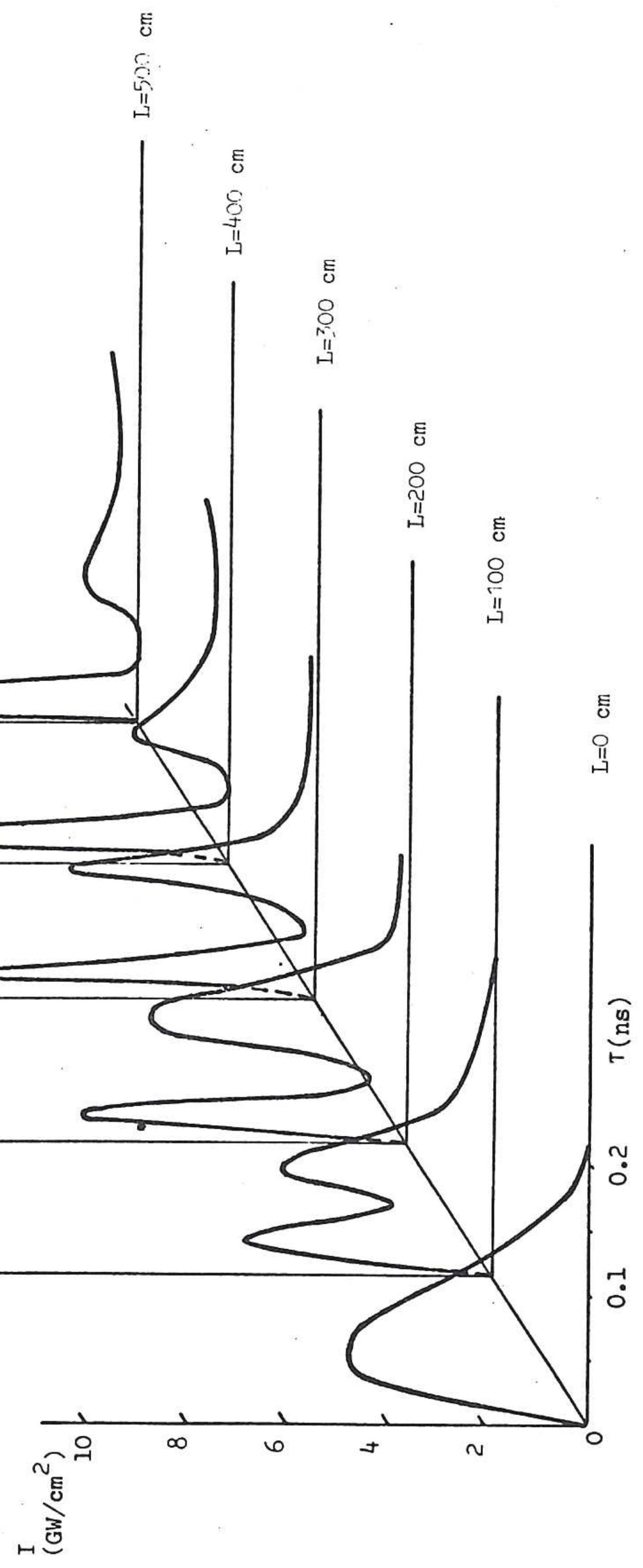

FIG.4 (a) Propagation of a stronger initial pulse than in Fig.3 (viz τ_o = 0.06 ns, I/P energy density 0.5 J/cm^2), showing the progressive development of a stationary pulse shape - having an ultimate area $\theta \sim 3\pi$.

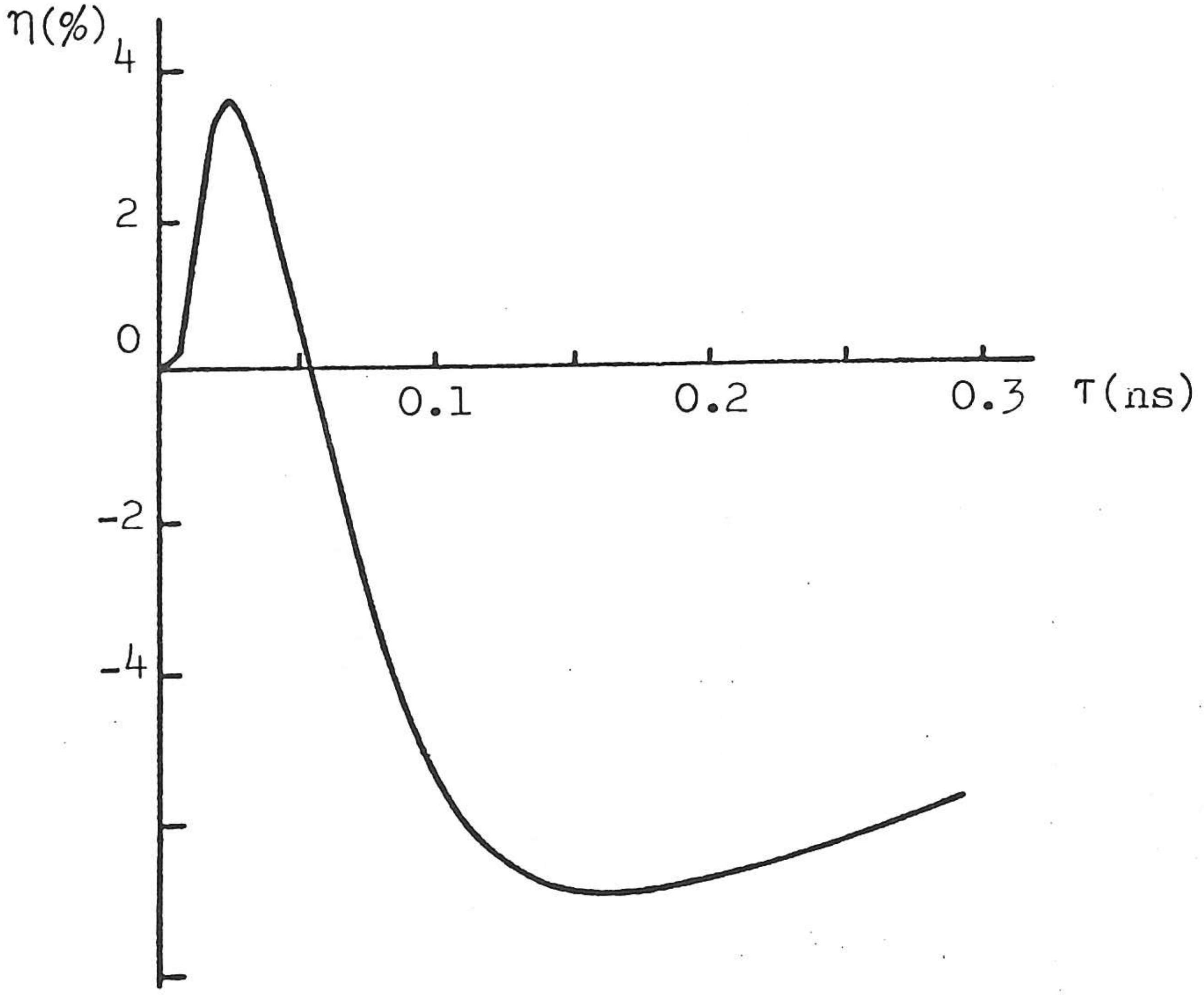

FIG.4 (b) Variation of η, at L = 5m, as a function of the retarded time τ.

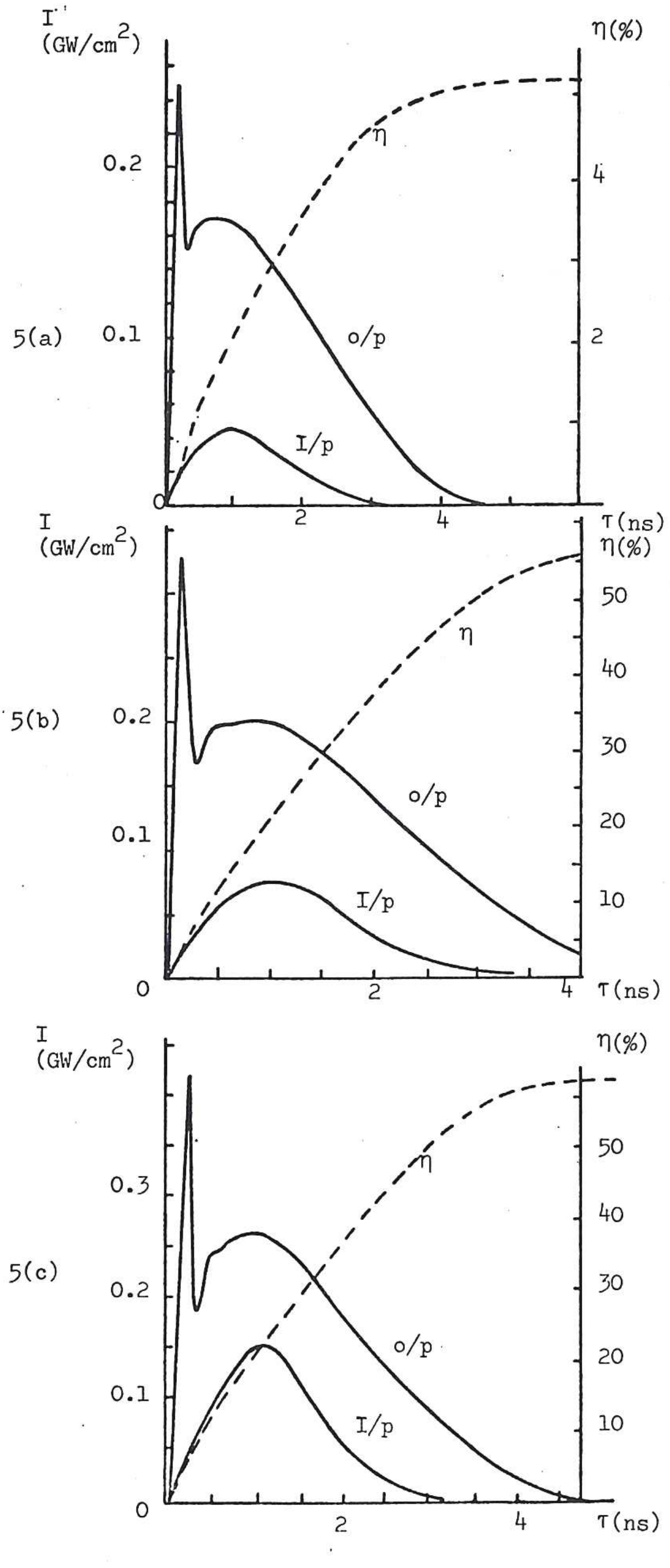

FIG.5 Plot similar to Fig.2, for τ_o = 1 ns (I/P energy densities (a) 0.075, (b) 0.125, (c) 0.25 J/cm^2).

6(a)

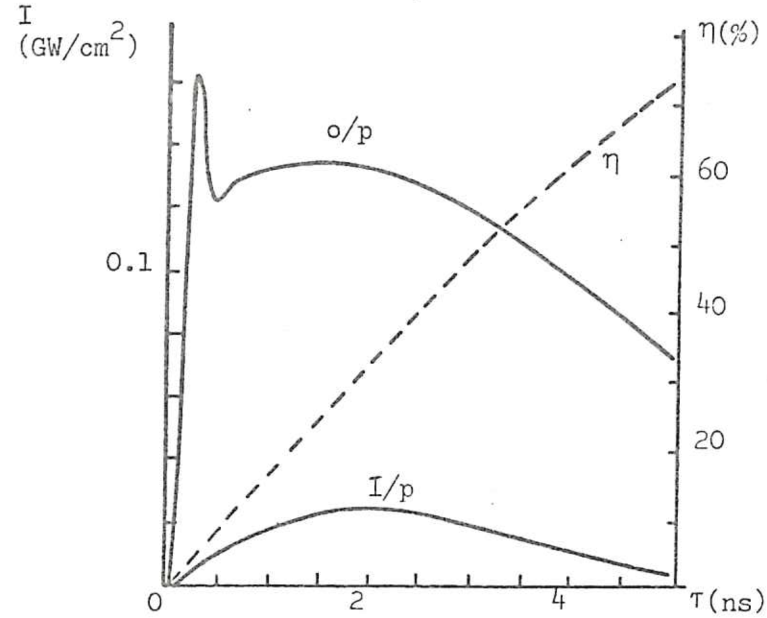

6(b)

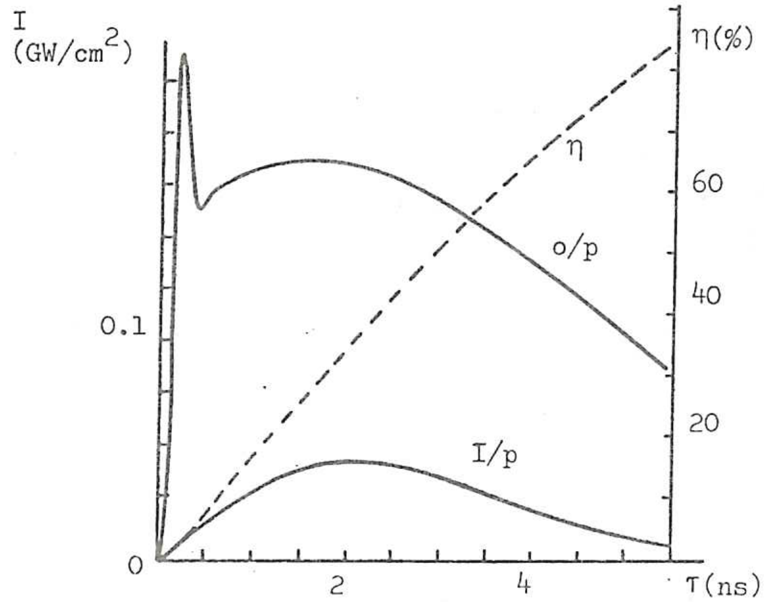

6(c)

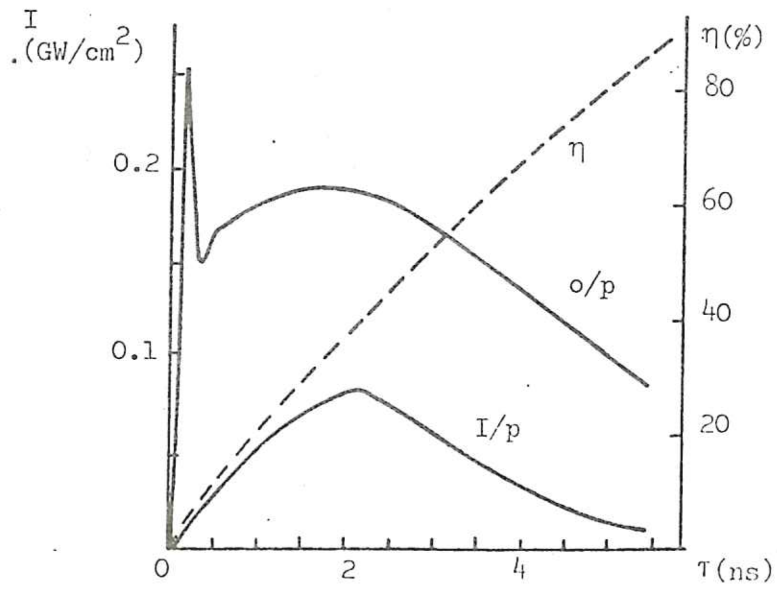

FIG.6 Plot similar to Fig.2, for τ_o = 2 ns. (I/P energy densities (a) 0.075, (b) 0.125, (c) 0.25 J/cm^2).

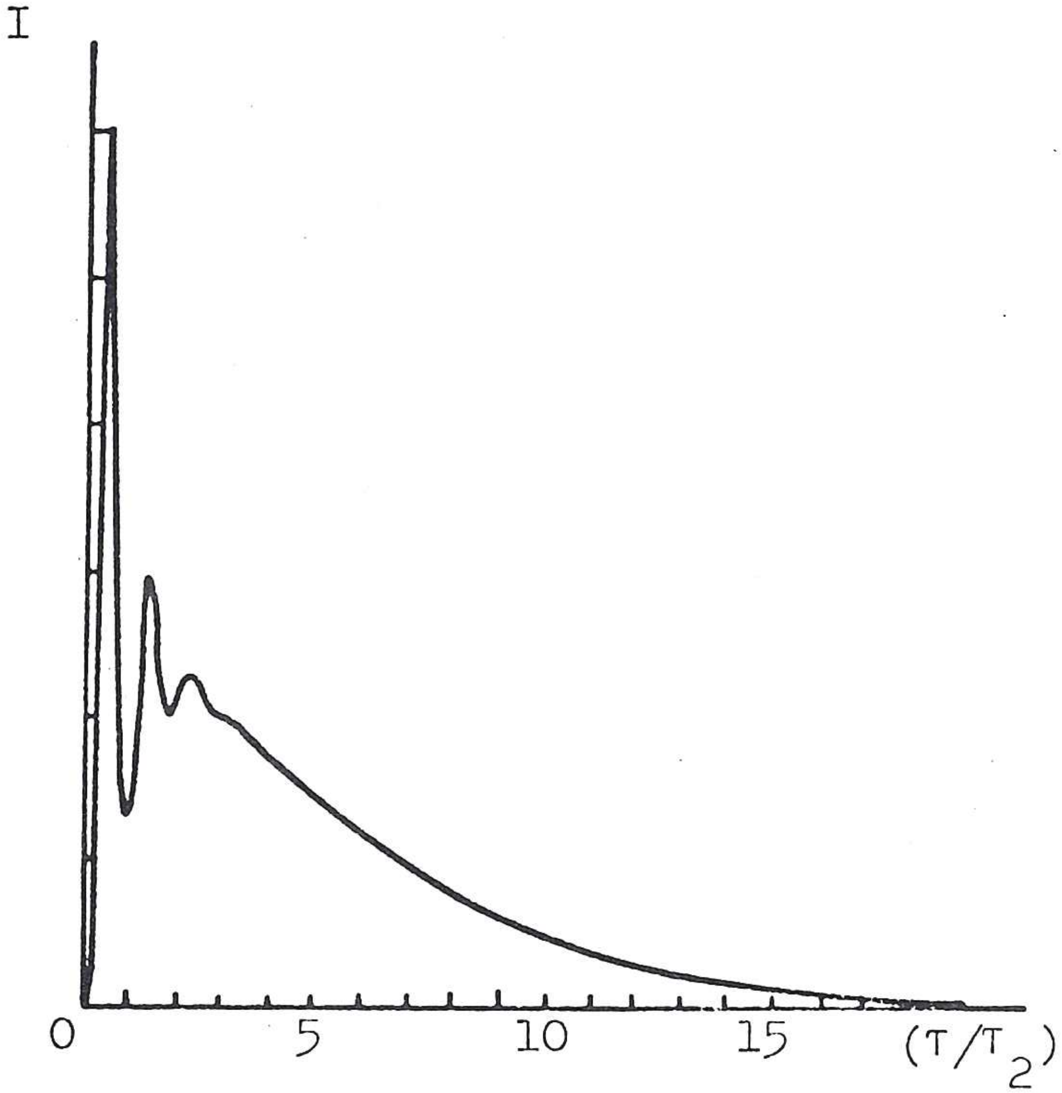

FIG.7 Fully developed asymptotic pulse, showing intensity (on a linear, but arbitrary, scale) after propagation of a $\tau_o = 1$ ns pulse along the high gain $\alpha_o = 0.05\ cm^{-1}$ amplifier of Fig.1 and Appendix 1. (NB Time normalized to the dipole-dephasing time τ_2.)